Study on the Release Behavior and Mechanism by Monitoring the Morphology Changes of the Large-Sized Drug-LDH Nanohybrids

Wei Huang, Hui Zhang, and Dengke Pan
State Key Laboratory of Chemical Resource Engineering, Beijing University of Chemical Technology, P.O. Box 98, Beijing 100029, China

DOI 10.1002/aic.12379
Published online August 13, 2010 in Wiley Online Library (wileyonlinelibrary.com).

Mg-Al layered double hydroxide (LDH) nanohybrids intercalated with ibuprofen (IBU) with particle sizes of 150–530 nm have been synthesized through hydrothermal and coprecipitation treatment in aqueous solution without any organic solvent. The in vitro drug release properties of as-prepared IBU-LDH nanohybrids are systematically studied and the kinetic simulation to the release profiles suggests that the release processes of the larger nanohybrids are mainly controlled by intraparticle diffusion. The morphology changes from thick sheet-like into thin margin-curved platelets for the larger nanohybrid particles, induced by the hydrophobic IBU anions aggregations located in the edge region of interlayer via ion-exchange diffusion process, is firstly observed during the release process. Based on the SEM, HRTEM, XRD, FTIR, and UV-vis analyses of the samples recovered at different release time, a release mechanism model of the as-prepared IBU-LDH nanohybrids is tentatively proposed along with their morphology changes during the whole release process. © 2010 American Institute of Chemical Engineers *AIChE J,* 57: 1936–1946, 2011
Keywords: drug-intercalated layered double hydroxide (LDH), large-sized nanohybrids, release mechanism, hydrophobic aggregation, margin-curved

Introduction

Recently, inorganic-based nanoparticles become a comparatively new focus of study for drug delivery and controlled-release agents.[1] Layered double hydroxides (LDHs), also known as hydrotalcite-like compounds with the general formula $[M^{2+}_{1-x}M^{3+}_{x}(OH)_2]^{x+}A^{n-}_{x/n}\cdot mH_2O$,[2,3] have exhibited extensive research interest in a number of areas, such as catalysis,[4–6] adsorption,[7,8] ion exchange,[4,9] and especially in drug delivery system as a novel biomaterials[1,10–12] due to their low cost, ease of preparation, ion-exchange property, low cytotoxicity, and high biocompatibility.[1,13,14] Ambrogi et al.[10] reported that the loosely flocculated ibuprofen (IBU)-intercalated Mg-Al-LDH nanoparticles (<200 nm) obtained by ion-exchange with chloride intercalated Mg-Al-LDH precursor showed almost 80% of IBU released only after 30 min ascribed to a dissolution mechanism. Zhang et al.[11] reported captopril intercalated Mg-Al-LDH by coprecipitation route and found that both the release rate and release percentages of captopril from the LDH nanocomposite were markedly decreased with increasing media pH from 4.60 to 7.45, attributing to the major dissolution mechanism and ion-exchange mechanism, respectively. Xu and coworkers[12] studied low molecular weight heparin (LMWH) intercalated Mg-Al-LDH and found that the release of LMWH from the LDH nanohybrids takes a much longer time compared with other drugs from LDH in pH 7–8 phosphate buffered

Additional Supporting Information may be found in the online version of this article.

Correspondence concerning this article should be addressed to H. Zhang at huizhang67@gst21.com.

solution (PBS),[10,11,15] because LMWH was multianionic species resulting in much stronger electrostatic interactions with the positively charged LDH layers. Evidently, the previous studies on drug-LDH hybrids are mainly focused on the synthesis, characterization, and in vitro release behavior, but less on the release mechanism with direct evidence through monitoring the whole release process of well-defined large-sized drug-LDH nanohybrid particles, thus approaching to the range of particle size suitable for drug delivery.[16]

Recently, Gunawan and Xu[17] claimed that the various aggregation states of the IBU-Mg-Al LDH particles, obtained by hydrothermal and coprecipitation step under varied solvent system and aging conditions, can impact the diffusion path length of IBU and thus the release rate, while no concern on the subtle influence of size and morphology of the single platelet particles. However, it is hard to illustrate the detailed release process and mechanism merely upon the morphology observations of the pristine sample and recovered one at the end of release test. To the best of our knowledge, there is no report on the detailed release process and release mechanism presented through scrutinizing the morphology and structure changes of the large-sized intercalates during the whole release process.

In this work, we investigate the release profiles of the large-sized drug-LDH nanohybrids involving widely used IBU as a model drug, obtained by hydrothermal method without any organic solvent, and firstly observe the changes of particle morphology and structure during the whole release process. A representative release mechanism model is tentatively proposed upon quasi-in-time SEM, HRTEM, XRD, FTIR, and UV-vis analyses, giving an insight into understanding the detailed release process and release mechanism of the drug from the LDH intercalates.

Experimental

IBU ($C_{13}H_{18}O_2$, MW 206) was purchased from the pharmaceutical factory of Juhua Group Corporation. $Mg(NO_3)_2{\cdot}6H_2O$ (AR) and $Al(NO_3)_3{\cdot}9H_2O$ (AR) were purchased from Beijing Yili Fine Chemical Company and NaOH (AR) from Beijing Beihua Fine Chemical Company. Decarbonated deionized water was employed by boiling and bubbling N_2 in all synthesis steps.

Synthesis of IBU-intercalated LDH nanohybrids

Large-sized IBU-intercalated Mg-Al-LDH nanohybrids were synthesized by hydrothermal method. An aqueous solution (100 ml) containing NaOH (0.08 mol) and IBU (0.015 mol) was added dropwise to a solution (65 ml) containing $Mg(NO_3)_2{\cdot}6H_2O$ (0.02 mol) and $Al(NO_3)_3{\cdot}9H_2O$ (0.01 mol) under N_2 atmosphere with vigorous stirring until the final pH 10. The resulting slurry was transferred and sealed into an autoclave, and then aged at 150°C for different aging time (18, 36, and 72 h). At the end of aging, the resultant was filtered, washed with water and ethanol until the pH ca. 7, and finally dried in vacuo at 60°C for 1 day. The obtained intercalates were named as MA-IBU-H-*i* (MA refers to Mg-Al-LDH, H to hydrothermal method, *i* (= 18, 36, and 72 h) to aging time). For comparison, a sample prepared by traditional coprecipitation step, i.e. the above resulting slurry was further aged at 70°C for 72 h under N_2 atmosphere with vigorous stirring instead of transferring into an autoclave, was obtained and named as MA-IBU-C (C refers to coprecipitation method).

In vitro drug release

The in vitro release of IBU from all intercalates were performed at 37 ± 1°C by adding ca. 50 mg samples into 250 ml simulated intestinal fluid (PBS at pH = 7.45) under a shaking speed of 50 rpm. The mass/volume ratio was chosen to simulate sink condition, according to the IBU solubility at this pH value.[10] A sample of 3 ml, which was then replaced by the same volume of PBS, was withdrawn at predetermined intervals and centrifuged for measuring the accumulated amount of IBU released using UV-vis spectrophotometer at λ_{max} = 221.0 nm. After release, the four samples were recovered, dried in vacuo at 60°C for 1 day, and denoted as MA-IBU-C-R and MA-IBU-H-*i*-R (R refers to the recovered sample, others the same as above), respectively, for subjecting to XRD, FTIR, UV-vis, SEM, and HRTEM characterizations.

To understand the release mechanism of IBU from the intercalates, five release kinetics models were used to fit the in vitro release profiles:[11,12,18–23] (1) The first-order model is applied extensively to the ion-exchange or adsorption process and can be expressed as: $\log(M_t/M_0) = -k_d \times t$; (2) The parabolic diffusion model is used to describe diffusion-controlled phenomena in soils and clays with the following equation: $(1 - M_t/M_0)/t = k_d \times t^{-0.5} + a$; (3) The modified Freundlich model explains experimental data on ion-exchange and diffusion-controlled process and can be written as: $\log(1 - M_t/M_0) = \log k_d + a\log t$; (4) The Elovich model is applied to chemisorption kinetics of ion-exchange adsorption on soils and clays: $1 - M_t/M_0 = a\ln t + b$; (5) The Bhaskar model can be used to evaluate whether the diffusion through the particle is the rate-limiting step and shown as: $\log(M_t/M_0) = -k_d \times t^{0.65}$.

In these models, M_0 and M_t represent the amount of IBU in LDH hybrids at release time of 0 and t, respectively, k_d the release rate constant, and a and b constants but their chemical significance is not clearly resolved.[12,18,23]

Characterization

Powder X-ray diffraction (XRD) patterns of all intercalates were obtained on a Shimadzu XRD-6000 powder X-ray diffractometer under the following conditions: 40 kV, 30 mA, Cu $K\alpha$ radiation (λ = 0.1542 nm) and scanning rate of 10°/min in the 2θ range of 2∼70°. Fourier-transformed infrared spectra (FTIR) were obtained on a Bruker Vector 22 spectrophotometer in the range of 4000∼400 cm^{-1} by using the standard KBr disk method (sample/KBr = 1/100). The UV absorption of IBU in solution and the UV-vis spectra of the samples were measured on a Shimadzu UV-2501PC spectrophotometer at λ_{max} = 221.0 nm and in the wavelength range of 200–500 nm, respectively. Metal elemental analysis was conducted by inductively coupled plasma emission spectroscopy (ICP) on a Shimadzu ICPS-7500 instrument. Contact angle (CA) was obtained through the Sessile Drop method using JC2000A contact angle/

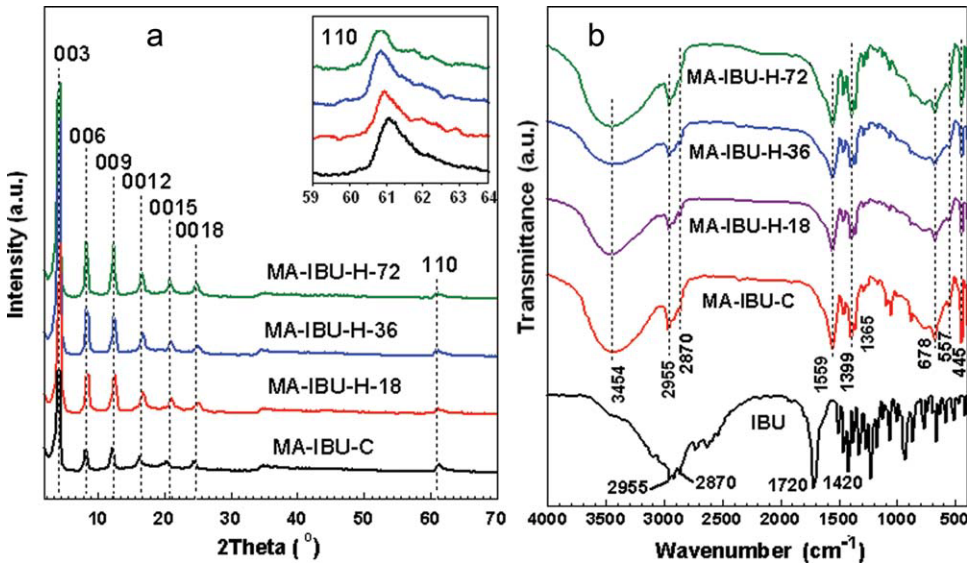

Figure 1. XRD (a) and FTIR (b) spectra of MA-IBU-C, MA-IBU-H-*i* samples and pure IBU.

[Color figure can be viewed in the online issue, which is available at wileyonlinelibrary.com.].

interface tensile measurer. The SEM micrograph was recorded on a Hitachi S-3500N scanning electron microscope. The TEM and HRTEM micrograph were obtained by Hitachi H-800 and JEOL JEM-2010 transmission electron microscope, respectively.

Results and Discussion

Crystal structure and morphology

The XRD patterns of the IBU intercalated LDH nanohybrids shown in Figure 1a indicate that all the intercalates possess the layered structure of LDH-like compounds indexed to the typical $3R_1$ polytype.[3,4,24] The highly ordered (003), (006), and (009), together with clear (0012), (0015), and (0018) diffractions of the MA-IBU-H-18, MA-IBU-H-36, and MA-IBU-H-72 are obviously sharper than those of MA-IBU-C, indicating that the hydrothermal treatments more favor the crystal growth than traditional coprecipitation one in the present drug-LDH system, similar to the observation in the synthesis of molecular sieves.[25] Table 1 shows the larger d_{003} values of 2.12~2.21 nm of the four intercalates than that of small inorganic-LDH such as NO_3^--LDH (0.88 nm),[4] implying the successful intercalation of large IBU anions in the interlayer region. The d_{110} values are slightly increased, along with the same trend of Mg/Al molar ratios (Table 1). It is carefully noted that the crystallinities of the MA-IBU-H-*i* hybrids are observably improved as the (110) line width is progressively decreased though their strengths almost unchanged with increasing aging time (Figure 1a inset), implying the gradually increased particle size as a function of aging time.

The FTIR spectra of all IBU-intercalated LDH nanohybrids (Figure 1b) clearly confirm the presence of IBU anions in the interlayer region. The formation of the LDH intercalates are demonstrated by a common broad band at 3454 cm^{-1} arising from the stretching mode of OH groups in the LDH layer and interlayer water as well as the sharp ones at 445, 557, and 678 cm^{-1} due to M—O and M—OH stretching vibrations in the LDH layer.[3] The bands at 2955 and 2870 cm^{-1} can be ascribed to C—H stretching mode of the intercalated IBU anions, quite close to that of IBU (Figure 1b). The antisymmetric and symmetric stretchings of COO^- group shift down to 1559 and 1399 cm^{-1} ($\Delta\nu = \nu_{as} - \nu_s =$ 160 cm^{-1}), instead of ν(C=O) for pure IBU with COOH group (1720 cm^{-1}), compared with those of IBU sodium (1584 and 1409 cm^{-1}),[26] indicating that the IBU anions within interlayer region probably bidentated linked with the host layer via hydrogen bonding between the COO^- group and hydroxylated LDH layer. An additional band at 1365

Table 1. Structural Parameters, Chemical Composition, and Release Data of the IBU Intercalated Hybrids

Samples	d_{003} (nm)	d_{110} (nm)	D (nm)*	Mg/Al†	IBU (%)‡	CA (°)§	$t_{50\%}$ (min)¶	Rel_{equ} (%)**
MA-IBU-C	2.210	0.1515	150	2.11	41.9	122.2	25	88
MA-IBU-H-18	2.122	0.1518	350	2.13	44.0	118.6	30	82
MA-IBU-H-36	2.165	0.1521	460	2.18	44.2	129.5	48	82
MA-IBU-H-72	2.194	0.1522	530	2.28	46.5	137.2	70	74

*Average particle size based on TEM results.
†Based on ICP analysis.
‡The drug loadings based on UV measurement.
§The shortened form of contact angle.
¶The time for 50% ibuprofen released from IBU-intercalated samples.
**The percentage of ibuprofen released at equilibrium.

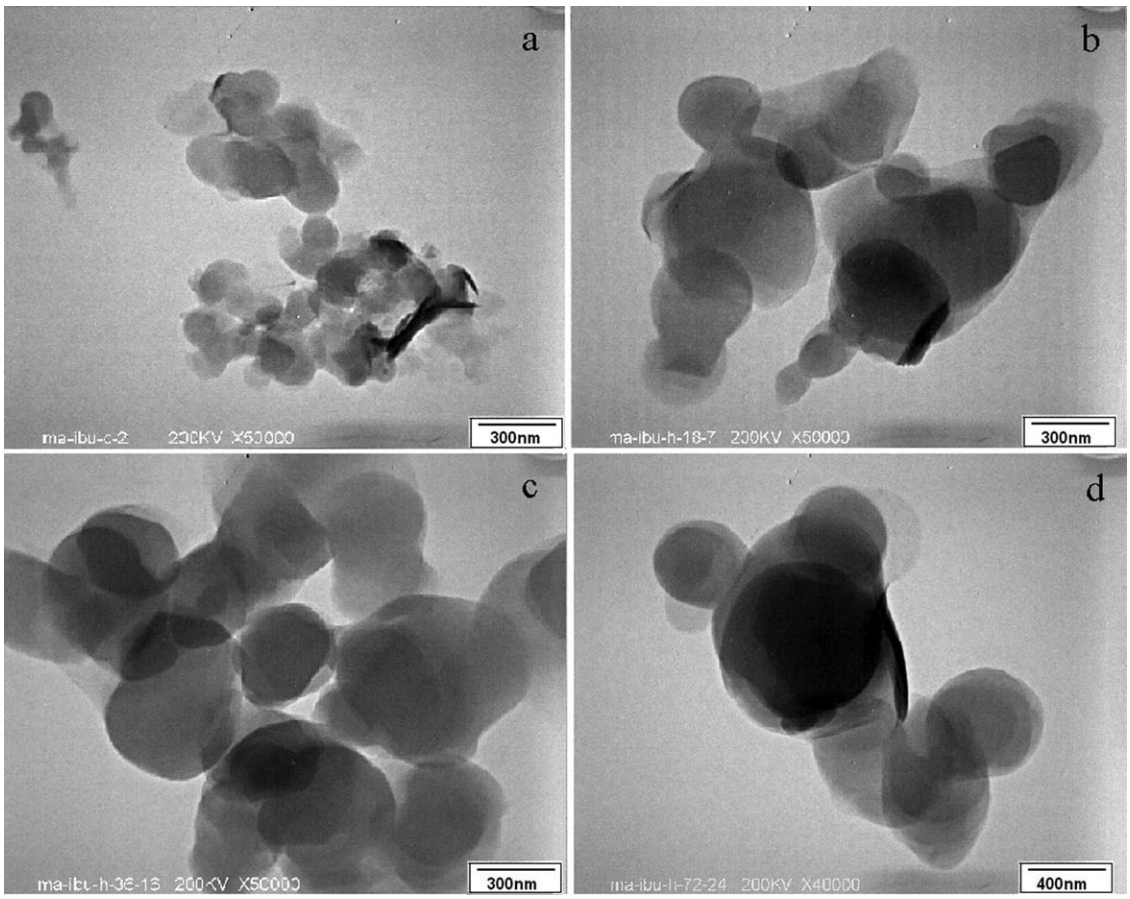

Figure 2. TEM images of MA-IBU-C (a) and MA-IBU-H-*i* samples (b–d refers to 18, 36, and 72 h).

cm^{-1} indicates some CO_3^{2-} contamination, which is difficult to exclude from LDH synthesis.[4,9,12] As for little variety among the FTIR spectra of all four samples, it suggests the similar host-guest interaction of the present IBU-LDH nanohybrids.

The TEM (Figure 2) and SEM (Figure 3) images show typical sheet-like morphology of all intercalates, and the round platelet particles orderly stacked and largely adhered to each other. This is the first report on round platelet-like large-sized IBU-LDH nanoparticles obtained in aqueous solution system, and the observed morphology is quite different from the previous reports.[10,17,27] It can be seen that the average particle size of MA-IBU-H-*i* nanohybrids is increased gradually from 350 to 530 nm, greatly larger than that of MA-IBU-C (~150 nm), with increasing aging time (Table 1), consistent with the XRD data. As Feng et al.[25,28] reported on hydrothermal and solvothermal synthetic chemistry and put forward that the reactivity in autoclave can be greatly improved under the high temperature and autocreated pressure when the solvent reached critical or supercritical state. Therefore, it can be understood that the hydrothermal method are more favored to the growth of the drug-LDH crystallite than coprecipitation one, and increasing aging time can further improve the growth of the particles. The TEM and SEM results show that all intercalates with average particle sizes in 150–530 nm have been prepared by varying operation parameters (synthesis routes and aging time).

In vitro drug release property

The IBU loadings of the obtained nanohybrids determined by UV measurement (Table 1) can be used to calculate the drug content in the samples before drug release studies and the in vitro release profiles of IBU from all intercalates in pH 7.45 PBS are shown in Figure 4. It can be seen that the particle size plays an important role on the release rate and equilibrium. Generally, IBU release from the present IBU-LDH nanohybrid particles takes a longer time than the previously reported drug-MgAl-LDH intercalates such as 90% of diclofenac[15] and 100% of IBU[10] released after 9 h and 100 min, respectively. The commonly observed incomplete release of the loaded drugs during in vitro release test of the drug-LDH hybrids is mainly due to the strong electrostatic interactions between the positively charged LDH layers and the negative charged drug anions in the LDH interlayer.[12,15] More importantly, the particle sizes of the present IBU-LDH nanohybrids are obviously larger than the reported IBU and diclofenac intercalated Mg-Al LDH, thus, the interlayer host-guest interaction sites and regions are relatively enhanced greatly and consequently result in prominent incomplete release behavior of IBU from the present IBU-

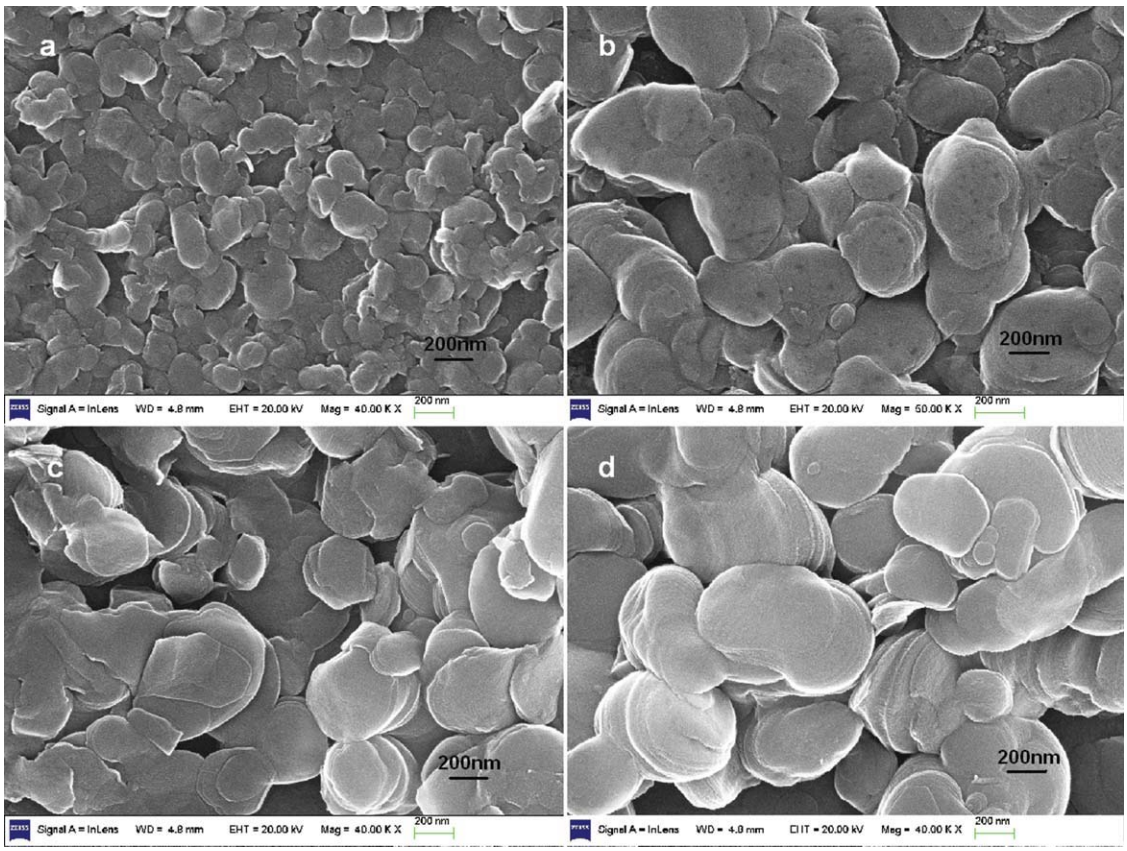

Figure 3. SEM images of MA-IBU-C (a) and MA-IBU-H-*i* samples (b–d refers to 18, 36, and 72 h).

[Color figure can be viewed in the online issue, which is available at wileyonlinelibrary.com.].

LDH nanohybrids. Moreover, the degree of the incomplete release is increased, and the release rates sequentially slow down with increasing particle sizes of MA-IBU-H-*i* nanohybrids. The time of 50% IBU released from MA-IBU-H-18, MA-IBU-H-36, and MA-IBU-H-72 are 30, 48, and 70 min, respectively, all higher than that of MA-IBU-C probably due to quite small particles of the coprecipitation sample (Table 1).

Five kinetic models were used to fit the release data (Table 2). Obviously, the first-order model is unsuitable to explain the release behavior of the four samples ($R^2 <$ 0.83), implying that the drug release is not a mainly dissolution determined process. From Figure 5, the modified Freundlich and Bhaskar models fit the release data of MA-IBU-H-36 and MA-IBU-H-72 better (R^2 in 0.91∼0.95), but less for MA-IBU-H-18 and MA-IBU-C ($R^2 < 0.87$), indicating that the release mechanism of the former two large-sized intercalates (>400 nm) may be controlled by ion exchange and particle diffusion processes,[18,22] dissimilar to the small-sized ones. The Elovich model describes a number of different processes including bulk and surface diffusion.[18] It is noted that Elovich model fits the release data of all four samples well (R^2 in 0.96∼0.99), implying that the release behavior of the intercalates with different particle sizes involve both bulk and surface diffusion processes.[18] As for the parabolic diffusion model, it fits the release data much better for MA-IBU-H-36 and MA-IBU-H-72 ($R^2 > 0.98$), good for MA-IBU-H-18 ($R^2 = 0.9287$) and poor for MA-IBU-C ($R^2 = 0.8318$). Together with the much smaller SD values compared to Elovich model (Table 2), it can be deduced that the parabolic diffusion model more fits to the whole release data for the larger intercalates (>400 nm), revealing that the release process of the guest IBU species through host lattice is controlled mainly by intraparticle diffusion,[12,18,22] though the release processes of all intercalates

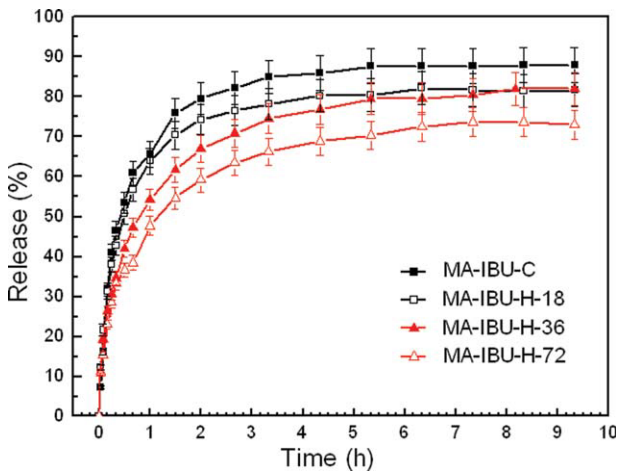

Figure 4. Release profiles of IBU from the MA-IBU-C (■), MA-IBU-H-18 (□), MA-IBU-H-36 (▲) and MA-IBU-H-72 (Δ) in pH 7.45 PBS.

[Color figure can be viewed in the online issue, which is available at wileyonlinelibrary.com.].

Table 2. The Linear Correlation Coefficients (R^2) and Standard Deviations (SD) upon Five Kinetic Models Fitting to the Release Data

Kinetic Models	Parameters	MA-IBU-C	MA-IBU-H-18	MA-IBU-H-36	MA-IBU-H-72
First-order	R^2	0.7397	0.7089	0.8291	0.8080
	SD	0.2714	0.2424	0.1806	0.1510
Parabolic diffusion	R^2	0.8318	0.9287	0.9857	0.9820
	SD	0.0051	0.0052	0.0019	0.0020
Modified Freundlich	R^2	0.8344	0.8683	0.9427	0.9468
	SD	0.1242	0.0820	0.0607	0.0590
Elovich	R^2	0.9649	0.9685	0.9861	0.9785
	SD	0.0512	0.0401	0.0289	0.0325
Bhaskar	R^2	0.8665	0.8390	0.9293	0.9141
	SD	0.1668	0.1590	0.1023	0.0891

involve the surface diffusion associated with their hydrophobic properties (Table 1, CA $>$ 110°).

The four samples were recovered after release test and dried at 60°C and subsequently submitted to XRD, FTIR, and SEM characterization. The XRD patterns of residual solids (Figure 6a) show that all the (003) peaks move to higher 2θ angle compared with the pristine intercalates (Figure 1a). The d_{003} of 0.83 nm for three MA-IBU-H-*i*-R samples and 0.88 nm for MA-IBU-C-R are observed probably owing to the fewer numbers of accessible sites around the edge of the larger intercalates and therefore needing more negatively HPO_4^{2-} than the smaller one,[29–31] confirming the intercalation of phosphate anions in the interlayer region during the release process combining with FTIR data (Figure 6b). From Figures 6a, b, it can be found that there are a few residual IBU anions within the interlayer regions (Figure 6a inset), consistent with the incomplete drug release of the hybrids at equilibrium (Table 1).

Figure 7 shows the SEM images of the recovered samples MA-IBU-H-*i*-R and MA-IBU-C-R. Quite interestingly, the margins of the samples are obviously curved with increasing particle sizes compared with the pristine sheet-like particles

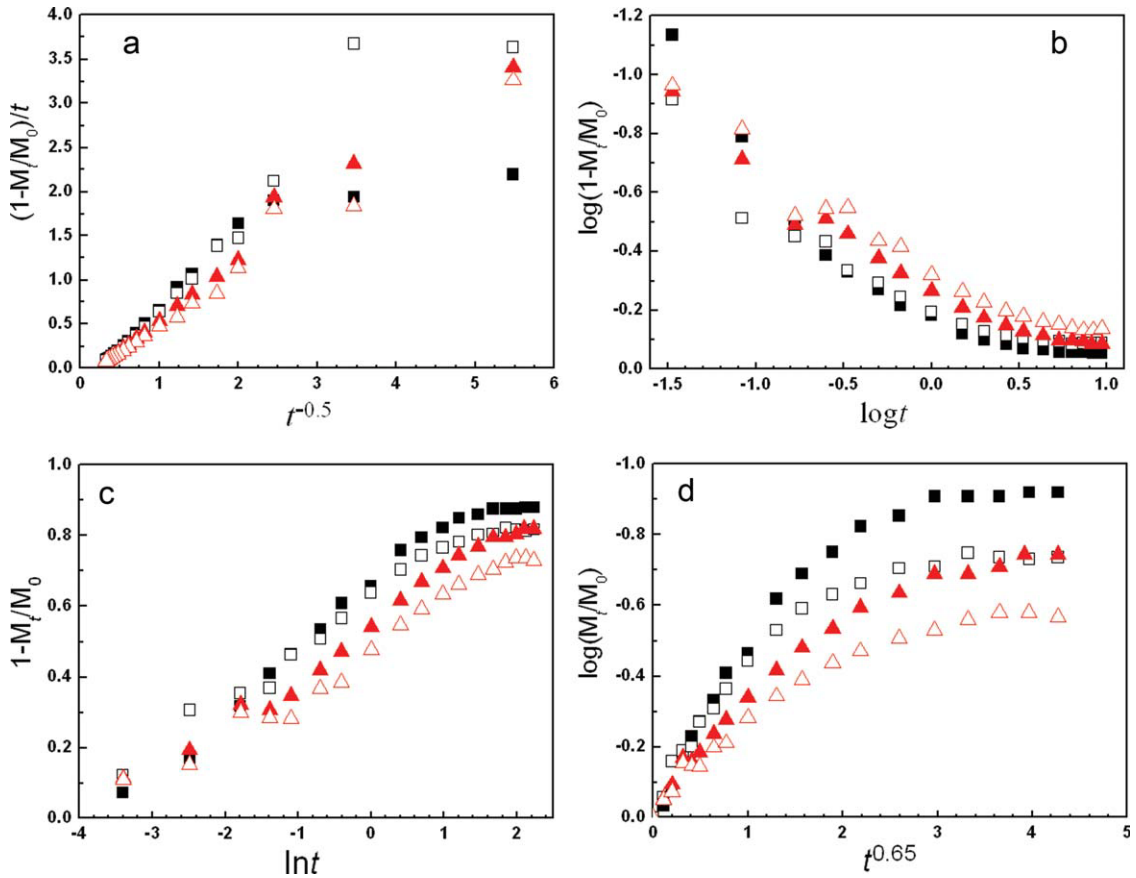

Figure 5. Plots of kinetic models of (a) parabolic diffusion model, (b) modified Freundlich model, (c) Elovich model, and (d) Bhaskar model for the release data of MA-IBU-C (■), MA-IBU-H-18 (□), MA-IBU-H-36 (▲) and MA-IBU-H-72 (Δ) in pH 7.45 PBS.

[Color figure can be viewed in the online issue, which is available at wileyonlinelibrary.com.].

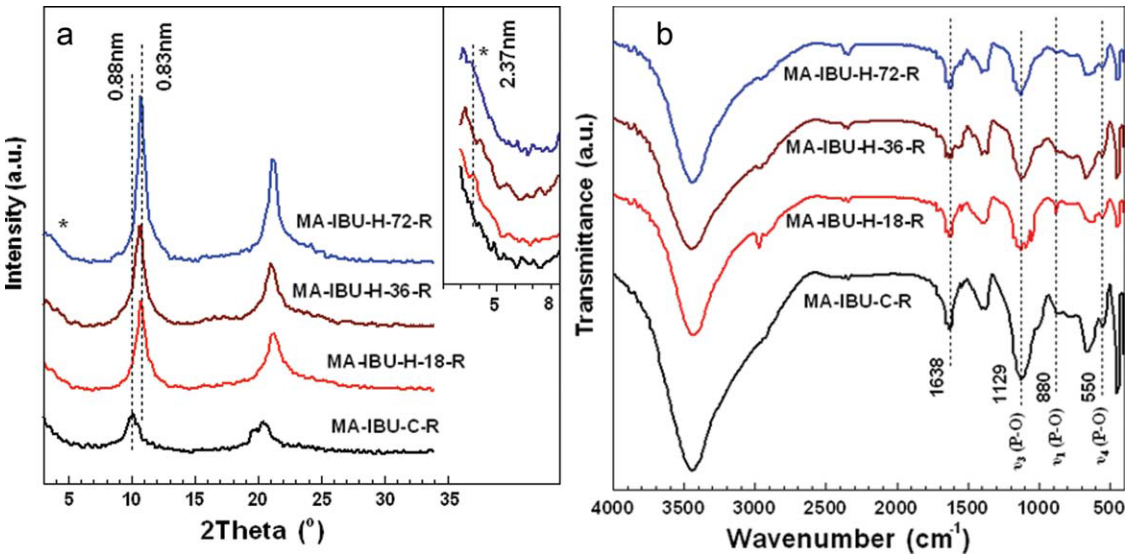

Figure 6. XRD (a) and FTIR (b) spectra of the recovered samples of MA-IBU-C-R and MA-IBU-H-*i*-R.

[Color figure can be viewed in the online issue, which is available at wileyonlinelibrary.com.].

(Figure 3). Ookubo et al.[32] previously published the small-sized (ca. 60 nm) plate-like phosphate- intercalated MgAl-LDH. Li and He[33] reported a sheet flexible SO_4^{2-}-LDH obtained during in situ decomposition of layer-bended dodecanesulfonate (DS)-LDH. Combining with the XRD and FTIR results of the recovered samples, it is believed that the large (~500 nm) margin-curved thin platelet-like phosphate intercalated LDH particles are obtained interestingly for the

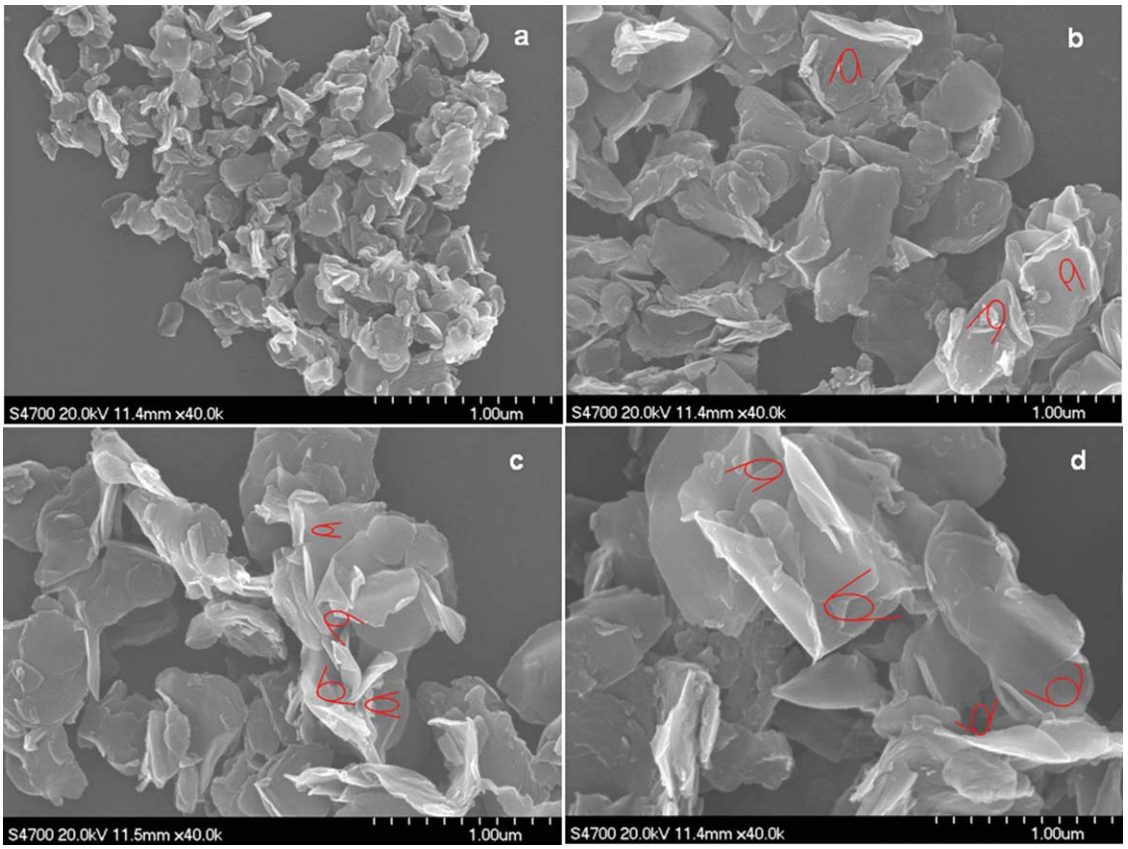

Figure 7. SEM images of the recovered samples MA-IBU-C-R (a) and MA-IBU-H-*i*-R (b–d refers to 18, 36, and 72 h) after in vitro release test in pH 7.45 PBS.

[Color figure can be viewed in the online issue, which is available at wileyonlinelibrary.com.].

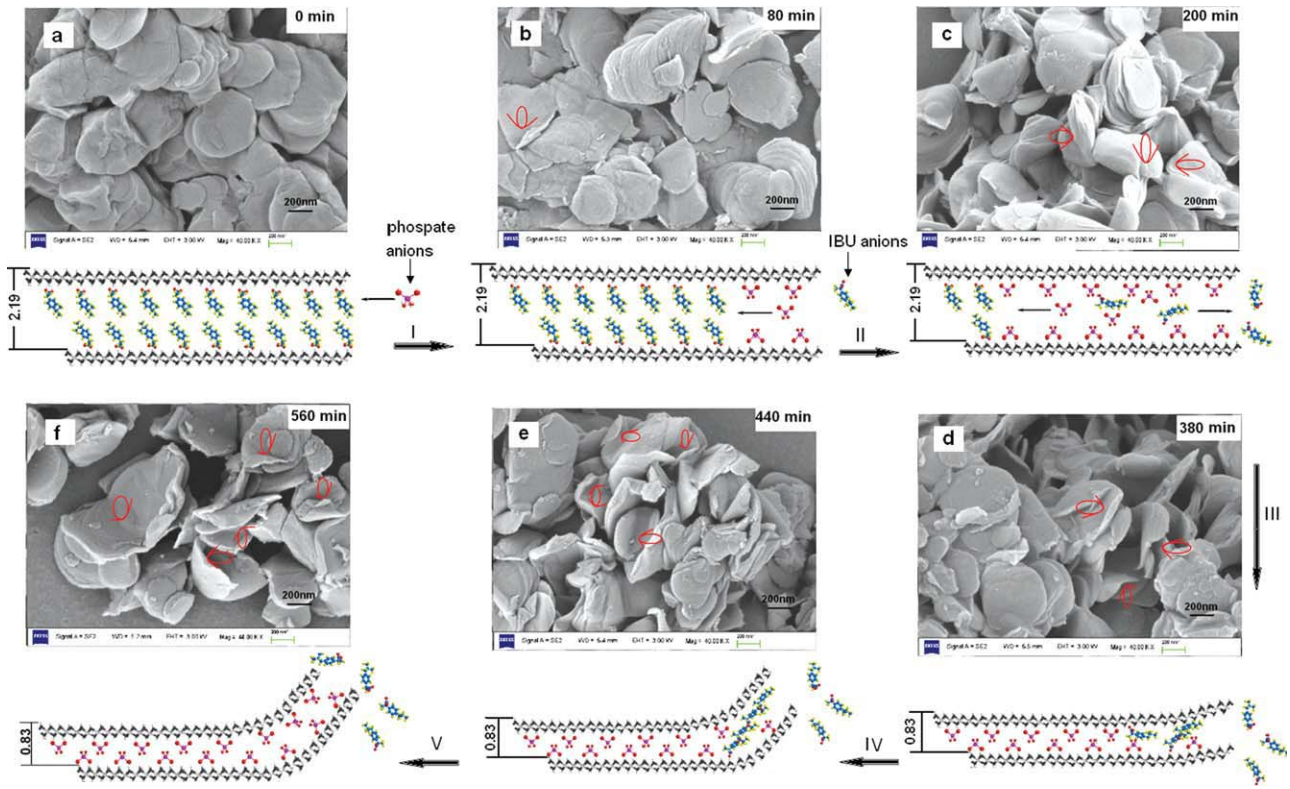

Figure 8. SEM images of the samples recovered at varied release time (a–f refers to 0, 80, 200, 380, 440, and 560 min) for the large-sized hybrid MA-IBU-H-72 with schematic representation of release mechanism associated to the morphology change during the release process.

[Color figure can be viewed in the online issue, which is available at wileyonlinelibrary.com.].

first time during the in vitro release process of the large-sized drug-LDH nanoparticles. This phenomenon has also been observed in IBU intercalated Zn-Al LDH system (Supporting Information, Figure S1). Therefore, it is worthy to further exploit the release process of the large-sized IBU-LDH nanohybrids by monitoring the samples recovered at different release time to provide detail elucidation of the release mechanism.

Release mechanism associated with the morphology change of the intercalates

To further investigate the release mechanism, we choose the largest sample MA-IBU-H-72 to quasi-in-time monitor the morphology changes resulting in curving process of the intercalate platelet-like particles. The SEM images in Figure 8 show the morphology of the recovered sample MA-IBU-H-72-R at different release time. At the beginning of in vitro release, the particles stack and adhere to each other seriously. During the release process from 0 to 200 min, the stacked particles gradually disperse, with the margins of the particles significantly beginning to curve at 80 min. When the release time arriving at 380 min, it tends to reach release equilibrium, and the particles almost completely disperse to the single one. From 380 to 560 min, it can be seen that the platelet-like particles bend more seriously with the increased amount of the curving particles.

The subsequent XRD and FTIR (Figures 9a, b) spectra of MA-IBU-H-72-R samples at different release time show that the amount of the intercalated IBU anions is gradually reduced, while that of the exchanged phosphate species is increased. At 380 min, the major phase of the recovered sample is the phosphate intercalated LDH, i.e., the amount of interlayer phosphate species is obviously more than that of IBU anions, and the IBU-LDH phase is hardly detected at 560 min by XRD analysis.

It can be seen from the UV-vis spectra (Figure 10) that the absorptions of $\pi \rightarrow \pi^*$ transition for pristine MA-IBU-H-72 nanohybrid at 225 nm are red shifted compared with pure IBU ($\sim$222 nm), implying the strong guest-guest interaction occurred via π-π function due to the highly ordered arrays of IBU anions in interlayer region.[9] With increasing release time, the absorptions at 225 nm become gradually weak due to the progressive release of the interlayer IBU anions and downshift to $\sim$221 nm owing to the slightly weakened guest-guest interaction. Up to 380 min, the absorption at 221 nm can be still observed, illustrating the existence of guest-guest hydrophobic aggregation of the interlayer exchanged IBU anions, which may result in the occurrence of the flexible margin-curved LDH particles as shown in Figure 8.

The further HRTEM images of the recovered MA-IBU-H-72-R samples (Figure 11) displays the obvious lattice fringes on the axis *c* of the LDH nanohybrids. The stacking of dark and light areas interphase can be clearly seen, similar to the previously report on organo-CaAl-LDH.[34,35] The dark areas

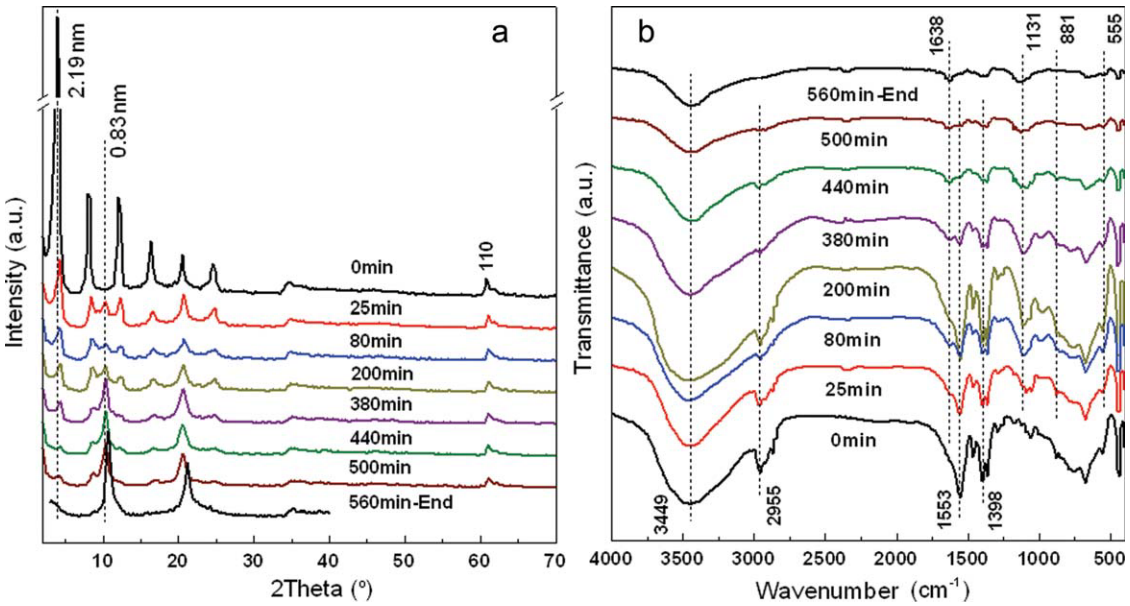

Figure 9. XRD (a) and FTIR (b) spectra of the samples recovered at varied release time for MA-IBU-H-72.

[Color figure can be viewed in the online issue, which is available at wileyonlinelibrary.com.].

represent the Mg-Al hydroxide layers, whereas the light ones represent the interlayer space intercalated by anions. From Figures 11a, c, it can be measured that the light areas represented the gallery height are 1.60∼1.75 nm at 0 min and 0.35∼0.40 nm at 560 min, respectively, in good agreement with the interlayer distance values from the XRD data (Figures 1a and 6a). However, from Figure 11b one can find a special gallery height of nearly 0.80∼0.90 nm at 380 min, between the values at 0 min and 560 min, indicating a special status of intercalation. It can be ascribed to incompletely release of interlayer IBU anions and the slightly remained guest-guest interactions among the exchanged IBU anions via hydrophobic interaction and π-π function near the edge region of the LDH interlayer, according to the XRD, FTIR (Figure 9), and UV-vis (Figure 10) data, which may largely afford to the curving of the large-sized IBU-LDH nanohybrids particles during the release process.

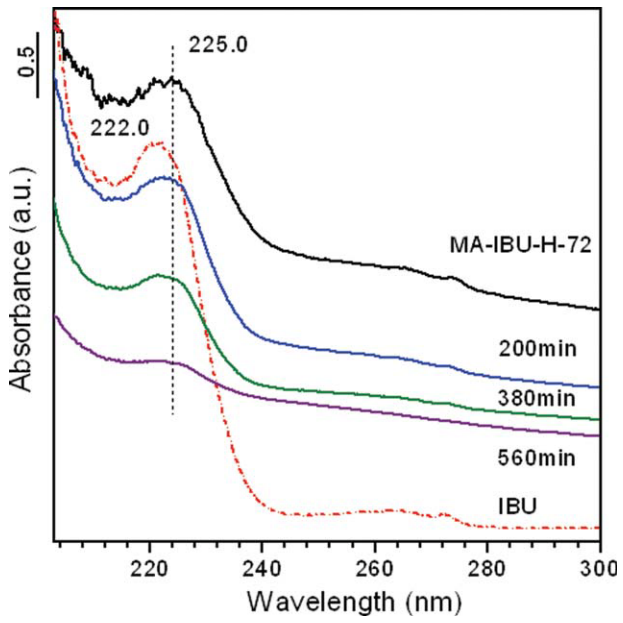

Figure 10. UV-vis absorption spectra of the samples recovered at 200, 380, and 560 min, compared with pristine MA-IBU-H-72 and pure IBU.

[Color figure can be viewed in the online issue, which is available at wileyonlinelibrary.com.].

Based on above results, it can be estimated that it is quite difficult for the exchanged IBU anions located in the centre of the interlayer domain to timely and completely diffuse into the PBS solution considering the longer diffusion path in line with the large-sized LDH plate-like particles. Consequently, the LDH layers may be forced to curve by the reoriented and aggregated interlayer IBU anions via hydrophobic interactions and π-π function, corresponding to the special status of the intercalation close to the interlayer gallery of 0.80∼0.90 nm as HRTEM revealed (Figure 11b). Therefore, we have tentatively proposed a release mechanism model to simulate the whole release process by following several steps involving the structure and morphology changes of the intercalates (Step I to V in Figure 8).

In Step I, the phosphate anions in PBS solution are gradually intercalated into the interlayer space by exchanging with the IBU anions at the edge of the intercalate particles. Interestingly, a dual orientation diffusion process presented in Step II, i.e., phosphate anions diffuse from the edge region into the middle of the two-dimensional LDH interlayer, and the IBU anions exchanged by the phosphate anions reorient and move out to the layer edged region and finally into the PBS solution, similar to the common ion-exchange process of the resinate and clays.[36,37] Factually in Step III, the IBU anions in the centre of the interlayer domain are almost completely exchanged by phosphate anions with a d_{003} reduced

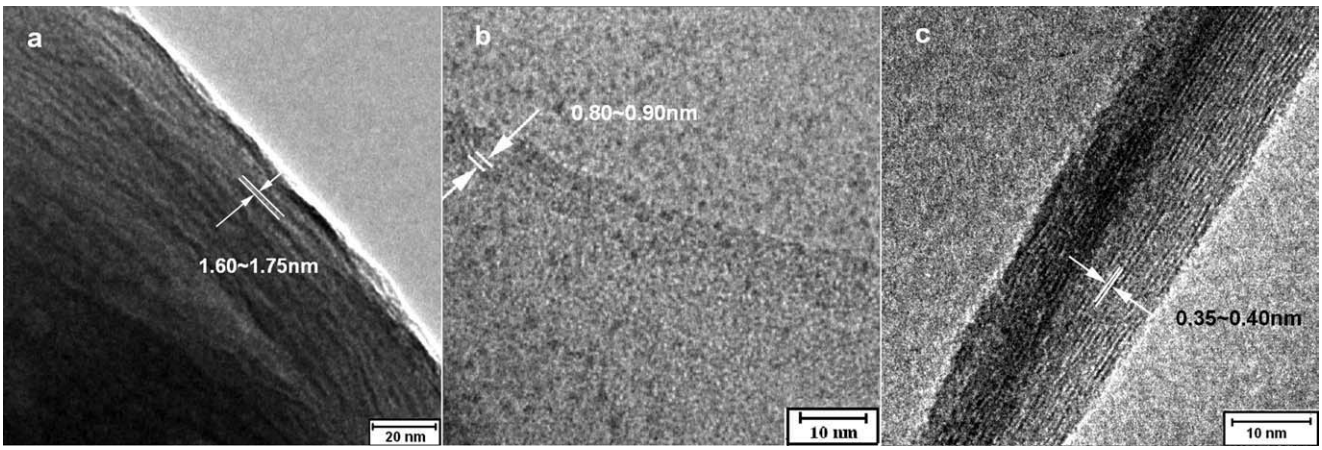

Figure 11. HRTEM images of the pristine MA-IBU-H-72 (a), and the samples recovered at 380 min (b) and 560 min (c).

from 2.19 to 0.83 nm, and the latter is quite close to the previously reported values of the phosphate intercalated LDH.[32] Although the exchanged IBU anions are largely released into the PBS solution, a few of IBU anions are still left in the edge region of the interlayer space and these residual IBU anions are more likely to aggregate due to the hydrophobic interaction from the phenyl ring and alkyl chain of IBU anions, and thereby generate a special force on the LDH layers, leading to the formation of margin-curved LDH particles. Then in Step IV, with increasing amount of the aggregated IBU anions, the force on the LDH layers become stronger and stronger and thus induce the particles bending more evidently. Finally in Step V, almost all the residual IBU anions are released to the PBS solution, and the margin-curved inorganic anion intercalated LDH material is remained. The proposed schematic representation (Figure 8) provides a clear illustration for the morphology and structure changes of the drug-LDH nanohybrids during the release process.

In summary, not only the length of two-dimensional semi-rigid LDH layers but also the morphology and structure changes of the intercalates during the release process is deemed to the key factor on the drug release rate and the diffusion mechanism. The interlayer aggregated hydrophobic drug anions can induce the intercalate particles curving through the hydrophobic force exerting on the LDH layers. This study indicates that the drug-LDH intercalates with different particle sizes approaching to the range of biological compatibility could be facilely synthesized by hydrothermal treatment without any organic agent and used as a kind of two-dimensional programmable container for drug molecules and the flexible drug-LDH nanohybrids may enable a novel potential route to fabricate different kinds of drug formulations such as suspension one.

Conclusions

The large-sized IBU-intercalated Mg-Al LDH nanohybrids with the particle size between 150–530 nm, approaching to the particle size range suitable for drug delivery, are successfully synthesized by hydrothermal and coprecipitation method without any organic solvent. The in vitro drug release in pH 7.45 PBS solution indicates that the release rate is sequentially reduced with increasing particle sizes of the intercalate particles. By quasi-in-time monitoring, the morphology changes of the large-sized drug-LDH during the release process, one can find that the pristine orderly stacked and largely adhered platelet drug-LDH nanoparticles are gradually changed into isolated and margin-curved thin plate-like LDH nanoparticles. The large-sized margin-curved phosphate intercalated LDH particles are obtained for the first time, implying a novel idea for synthesizing margin-curved inorganic-LDH intercalates. The main reason leading to margin-curved LDH particles is the hydrophobic aggregation mechanism of the interlayer exchanged hydrophobic IBU anions. This result has a potential significance to the studies on drug release behavior and mechanism of other drug-LDH systems and provides a potential route to fabricate different kinds of drug formulations.

Acknowledgments

We are grateful to the financial support from the National Natural Science Foundation of China (20776012), 111 Project (B07004), National Science and Technology Pillar Program (2009BAE89B01) and 973 Program (2009CB939802).

Literature Cited

1. Faraji AH, Wipf P. Nanoparticles in cellular drug delivery. *Bioorg Med Chem*. 2009;17:2950–2962.
2. Khan AI, O'Hare D. Intercalation chemistry of layered double hydroxides: recent developments and applications. *J Mater Chem*. 2002;12:3191–3198.
3. Evans DG, Duan X. Preparation of layered double hydroxides and their applications as additives in polymers, as precursors to magnetic materials and in biology and medicine. *Chem Commun*. 2006;6:485–496.
4. Cavani F, Trifiro F, Vaccari A. Hydrotalcite-type aninic clays: preparation, properties and applications. *Catal Today*. 1991;11:173–301.
5. Tichit D, Lutic D, Coq B, Durand R, Teissier R. The aldol condensation of acetaldehyde and heptanal on hydrotalcite-type catalysts. *J Catal*. 2003;219:167–175.
6. Lei XD, Zhang FZ, Yang L, Guo XX, Tian YY, Fu SS, Li F, Evans DG, Duan X. Highly crystalline activated layered double hydroxides as solid acid-base catalyst. *AIChE J*. 2007;4:932–940.
7. Mezenner NY, Bensmaili A. Kinetics and thermodynamic study of phosphate adsorption on iron hydroxide-eggshell waste. *Chem Eng J*. 2009;147:87–96.
8. Islam H, Patel R. Nitrate sorption by thermally activated Mg/Al chloride hydrotalcite-like compound. *J Hazard Mater*. 2009;1692:524–531.
9. Zou K, Zhang H, Duan X. Studies on the formation of 5-aminosalicylate intercalated Zn–Al layered double hydroxides as a function of

Zn/Al molar ratios and synthesis routes. *Chem Eng Sci*. 2007;62: 2022–2031.
10. Ambrogi V, Fardella G, Grandolini G, Perioli L. Intercalation compounds of hydrotalcite-like anionic clays with antiinflammatory agents—I. Intercalation and in vitro release of ibuprofen. *Int J Pharm*. 2001;220:23–32.
11. Zhang H, Zou K, Guo SH, Duan X. Nanostructural drug-inorganic clay composites: structure, thermal property and in vitro release of captopril-intercalated Mg–Al-layered double hydroxides. *J Solid State Chem*. 2006;179:1792–1801.
12. Gu Z, Thomas AC, Xu ZP, Campbell JH, Lu GQ. In vitro sustained release of LMWH from MgAl-layered double hydroxide nanohybrids. *Chem Mater*. 2008;20:3715–3722.
13. Choy JH, Choi SJ, Oh JM, Park T. Clay minerals and layered double hydroxides for novel biological applications. *Appl Clay Sci*. 2007;36:122–132.
14. Xu ZP, Niebert M, Porazik K, Walker TL, Cooper HM, Middelberg APJ, Gray PP, Bartlett PF, Lu GQ. Subcellular compartment targeting of layered double hydroxide nanoparticles. *J Control Release*. 2008;130:86–94.
15. Ambrogi V, Fardella G, Grandolini G, Perioli L, Tiralti MC. Intercalation compounds of hydrotalcite-like anionic clays with anti-inflammatory agents, II: uptake of diclofenac for a controlled release formulation. *AAPS PharmSci*. 2002;3:article 26,1–6.
16. Xu ZP, Stevenson G, Lu CQ, Lu GQ. Dispersion and size control of layered double hydroxide nanoparticles in aqueous solution. *J Phys Chem B*. 2006;110:16923–16929.
17. Gunawan P, Xu R. Direct control of drug release behavior from layered double hydroxides through particle interactions. *J Pharm Sci*. 2008;97:4367–4378.
18. Yang JH, Han YS, Park M, Park T, Hwang SJ, Choy JH. New inorganic-based drug delivery system of indole-3-acetic acid-layered metal hydroxide nanohybrids with controlled release rate. *Chem Mater*. 2007;19:2679–2685.
19. Kodama T, Harada Y, Ueda M, Shimizu K, Shuto K, Komarneni S. Selective exchange and fixation of strontium ions with ultrafine Na-4-mica. *Langmuir*. 2001;17:4881–4886.
20. Li ZH. Sorption kinetics of hexadecyltrimethylammonium on natural clinoptilolite. *Langmuir*. 1999;15:6438–6445.
21. Low MJD. Kinetics of chemisorption of gases on solids. *Chem Rev*. 1960;60:267–312.
22. Zhang H, Pan DK, Zou K, He J, Duan X. A novel core-shell structured magnetic organic-inorganic nanohybrid involving drug-intercalated layered double hydroxides coated on a magnesium ferrite core for magnetically controlled drug release. *J Mater Chem*. 2009;19:3069–3077.
23. Zhang H, Pan DK, Duan X. Synthesis, characterization, and magnetically controlled release behavior of novel core-shell structural magnetic ibuprofen-intercalated LDH nanohybrids. *J Phys Chem C*. 2009;113:12140–12148.
24. Xu ZP, Lu GQ. Hydrothermal synthesis of layered double hydroxides (LDHs) from mixed MgO and Al_2O_3: LDH formation mechanism. *Chem Mater*. 2005;17:1055–1062.
25. Feng SH, Xu RR. New materials in hydrothermal synthesis. *Acc Chem Res*. 2001;34,239–247.
26. Rodriguez R, Alvarez-Lorenzo C, Concheiro A. Interactions of ibuprofen with cationic polysaccharides in aqueous dispersions and hydrogels rheological and diffusional implications. *Eur J Pharm Sci*. 2003;20:429–438.
27. Gunawan P, Xu R. Synthesis of unusual coral-like layered double hydroxide microspheres in a nonaqueous polar solvent/surfactant system. *J Mater Chem*. 2008;12:2112–2120.
28. Feng SH. Hydrothermal and solvothermal synthetic chemistry. *J Jilin Norm Univ (Nat Sci Ed)*. 2008;3:7–11.
29. Costantino U, Casciola M, Massinelli L, Nocchetti M, Vivani R. Intercalation and grafting of hydrogen phosphates and phosphonates into synthetic hydrotalcites and a.c.-conductivity of the compounds thereby obtained. *Solid State Ionics*. 1997;97:203–212.
30. Badreddine M, Khaldi M, Legrouri A, Barroug A, Chaouch M, De Roy A, Besse JP. Chloride-hydrogenophosphate ion exchange into the zinc-aluminum-chloride layered double hydroxide. *Mater Chem Phys*. 1998;52:235–239.
31. Khaldi M, Badreddine M, Legrouri A, Chaouch M, Barroug A, De Roy A, Besse JP. Preparation of a well-ordered layered nanocomposite from zinc-aluminum- chloride layered double hydroxide and hydrogenophosphate by ion exchange. *Mater Res Bull*. 1998;33: 1835–1843.
32. Ookubo A, Ooi K, Hayasi H. Preparation and phosphate ion-exchange properties of a hydrotalcite-like compound. *Langmuir*. 1993;9:1418–1422.
33. Li B, He J. Multiple effects of dodecanesulfonate in the crystal growth control and morphosynthesis of layered double hydroxides. *J Phys Chem C*. 2008;112:10909–10917.
34. Plank J, Keller H, Andres PR, Dai Z. Novel organo-mineral phases obtained by intercalation of maleic anhydride-allyl ether copolymers into layered calcium aluminum hyrates. *Inorg Chim Acta*. 2006;359: 4901–4908.
35. Plank J, Dai Z, Andres PR. Preparation and characterization of new Ca-Al- polycarboxylate layered double hydroxides. *Mater Lett*. 2006;60:3614–3617.
36. Park JK, Choy YB, Oh JM, Kim JY, Hwang SJ, Choy JH. Controlled release of donepezil intercalated in smectite clays. *Int J Pharm*. 2008;359:198–204.
37. Anand V, Kandarapu R, Garg S. Ion-exchange resins: carrying drug delivery forward. *Drug Discov Today*. 2001;17:905–914.

Manuscript received Apr. 23, 2010, and revision received July 6, 2010.